

Dijets at the EIC beyond TMDs

Farid Salazar
November 16th, 2021

R. Boussarie, H. Mäntysaari, FS, and B. Schenke. [2106.11301](#) (JHEP09(2021)178)

P. Caucal, FS, and R. Venugopalan. [2108.06347](#) (To appear on JHEP)

UCLA



Berkeley
UNIVERSITY OF CALIFORNIA

Outline

- Dijet production in the TMD formalism
Observables at the EIC
- Dijet production at EIC beyond TMDs
Resummation of kinematic and genuine saturation corrections
- Dijet production at EIC in the CGC at NLO
JIMWLK rapidity factorization, and finite impact factor
- Outlook

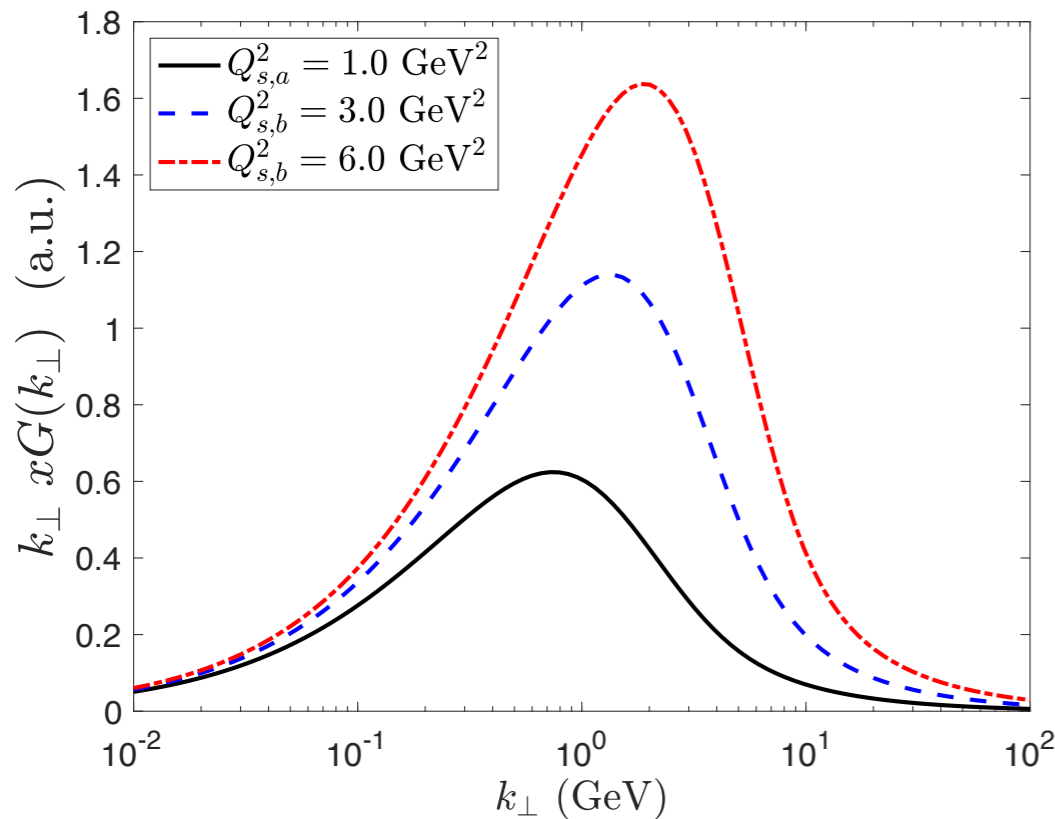
Dijet and dihadron production: TMD formalism

Forward dihadron azimuthal correlations and gluon saturation

Weizsäcker-Williams TMD
at small- x

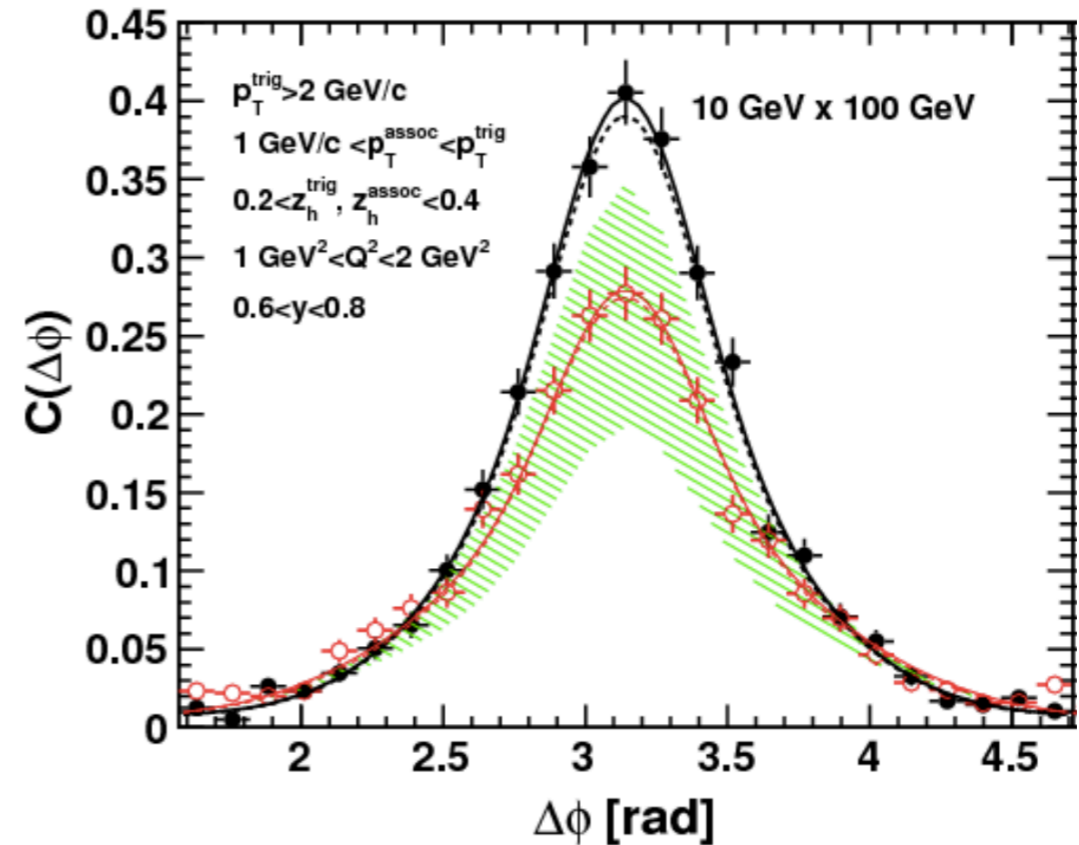


Dihadron suppression
back-to-back peak

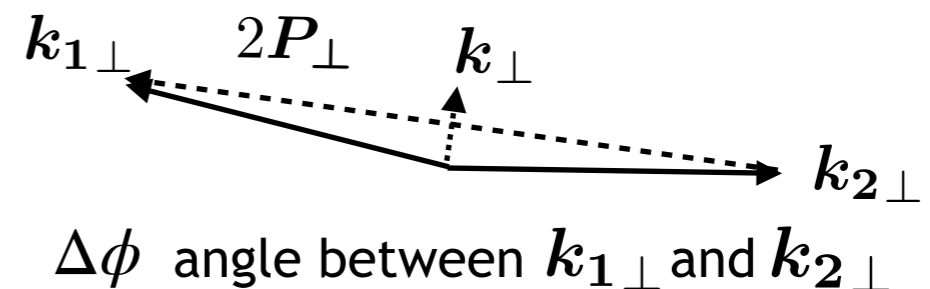


Typical momentum transfer from
hadron/nucleus to

Momentum imbalance $\longrightarrow k_{\perp} \sim Q_s \longleftarrow$ Saturation scale



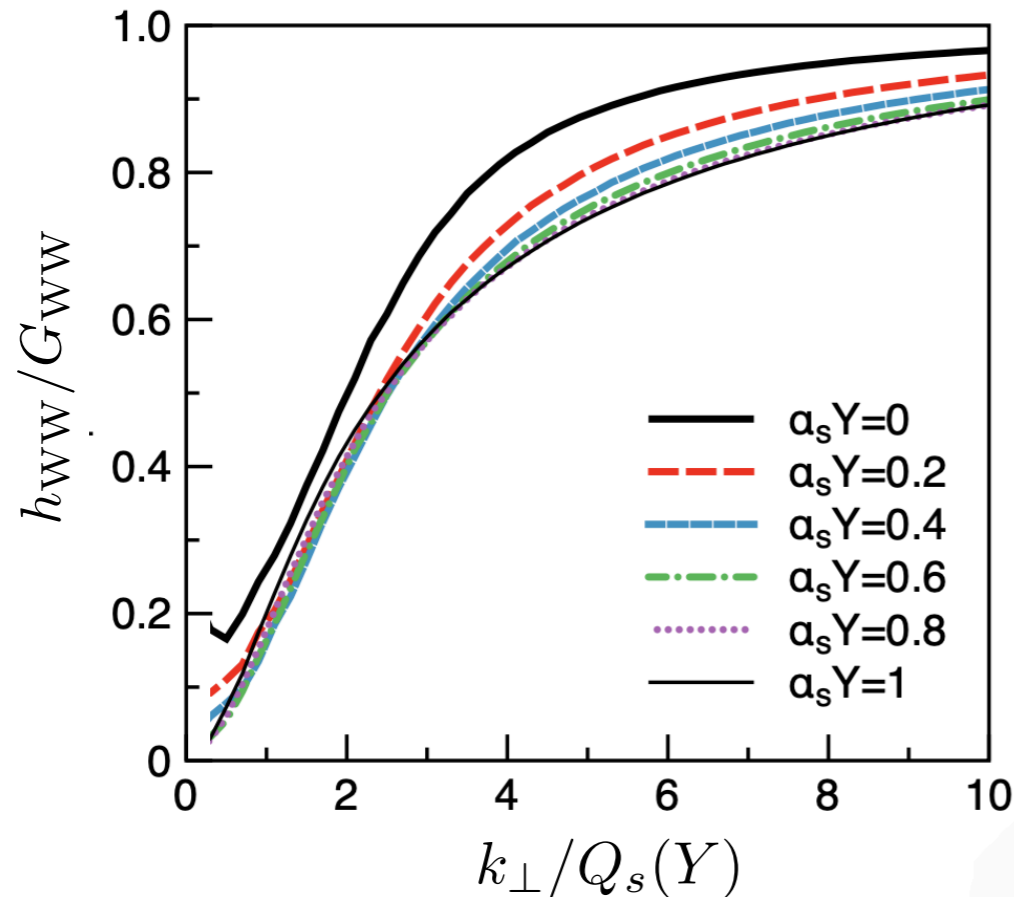
Zheng, Aschenauer, Lee, Xiao (2014)



Dijet and dihadron production: TMD formalism

Forward dijet azimuthal asymmetries and linearly pol WW gluon TMD

Ratio of linearly polarized to unpolarized gluon WW



Dumitru, Lappi, Skokov (2015)

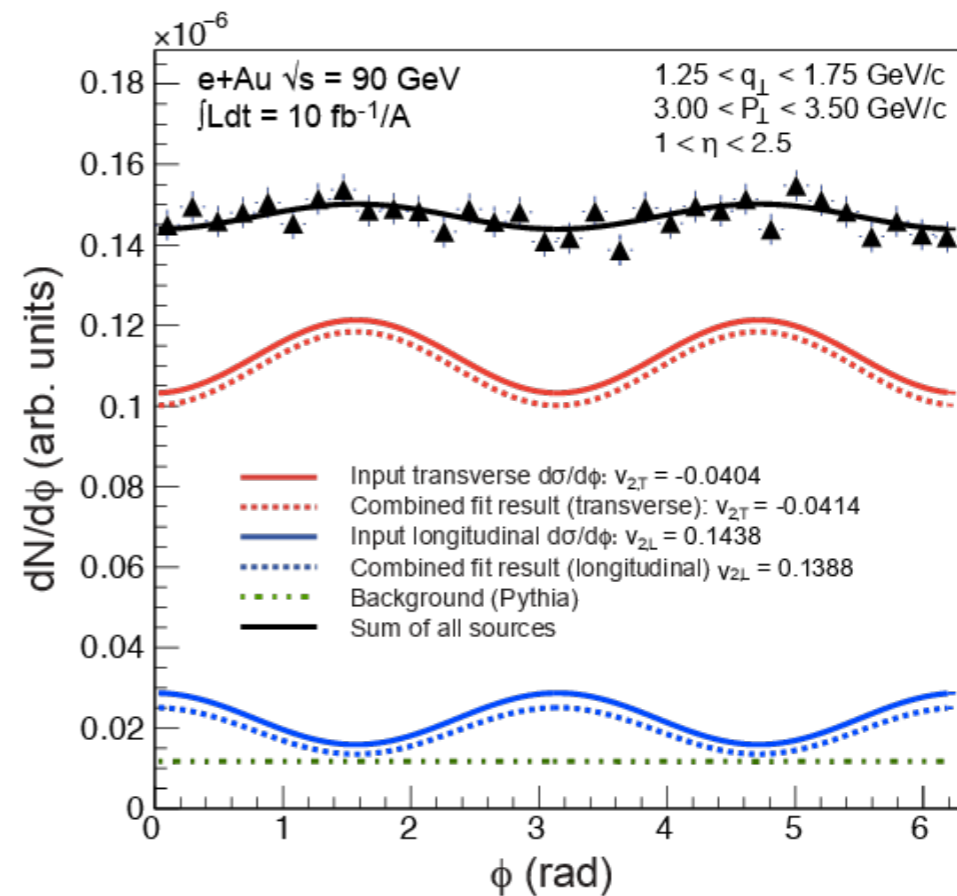
Accessed in azimuthal asymmetry of momentum imbalance in dijet pairs

Dominguez, Qiu, Xiao, Yuan (2011)

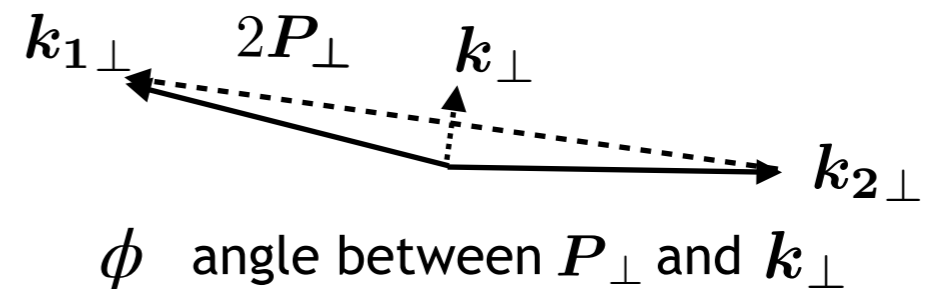
See Feng's talk tomorrow
effects of soft gluon radiation!



Dijet azimuthal asymmetries in momentum imbalance

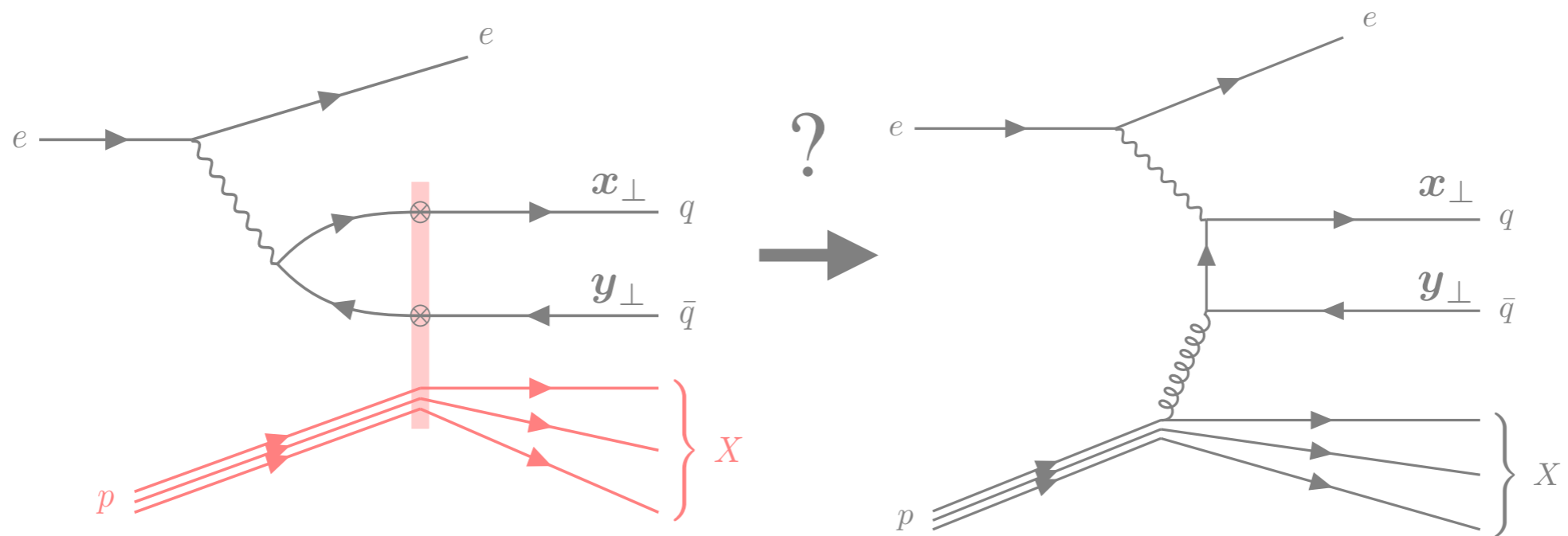


Dumitru, Skokov, Ullrich (2018)



$$|v_2| \sim \frac{x h_{WW}}{x G_{WW}}$$

Dijet production beyond TMDs



A comprehensive numerical study of the TMD/CGC correspondence

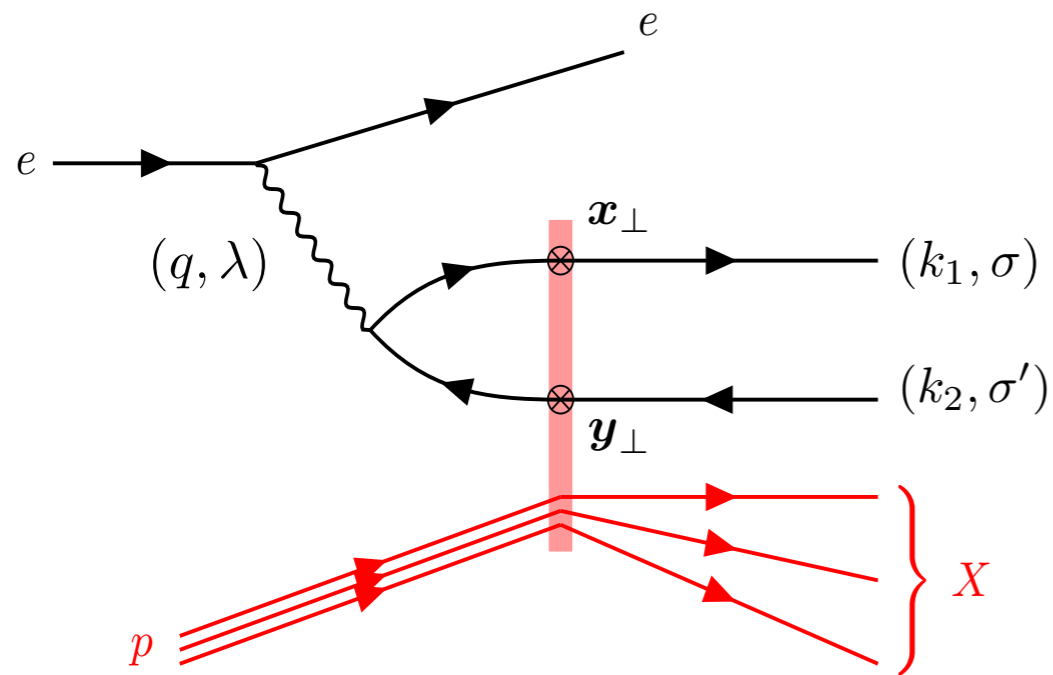
R. Boussarie, H. Mäntysaari, FS, and B. Schenke. [2106.11301](#) (JHEP09(2021)178)



Dijet production beyond TMDs

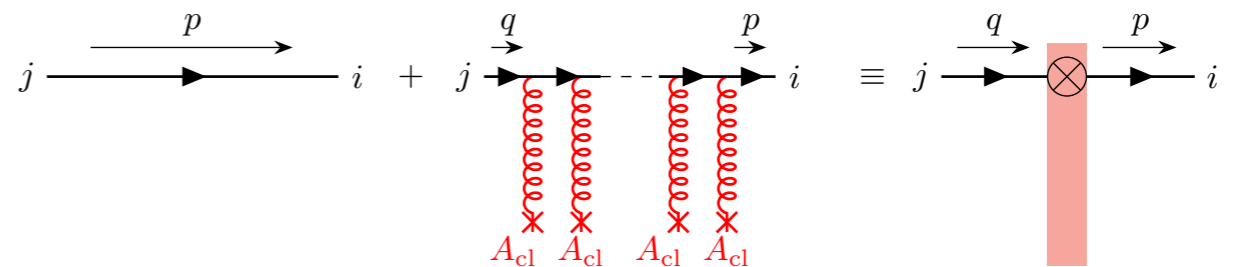
Computation in the CGC: resummation of multiple scatterings

Dominguez, Marquet, Xiao, Yuan (2011)



LO diagram for $q\bar{q}$ production in the CGC EFT

Dense gluon field $A_{cl} \sim 1/g$ needs resummation of multiple gluon interactions



$$V_{ij}(\mathbf{x}) = P \exp \left\{ ig \int dx^- A_{cl}^{+,a}(\mathbf{x}, x^-) t^a \right\}$$

Amplitude (modulo leptonic part):

$$\mathcal{M}_{LO}^{\lambda\sigma\sigma'} = \underbrace{\Psi \gamma_{\lambda}^* \rightarrow q\bar{q}(Q, \mathbf{r}_{xy}, z_q)}_{\text{perturbatively computable}} \otimes_{LO} \underbrace{[1 - V(\mathbf{x}_{\perp})V^{\dagger}(\mathbf{y}_{\perp})]}_{\text{non-perturbative}}$$

$$\otimes_{LO} \equiv \frac{ee_f q^-}{\pi} \int d^2\mathbf{x}_{\perp} d^2\mathbf{y}_{\perp} e^{-i\mathbf{k}_{1\perp} \cdot \mathbf{x}_{\perp}} e^{-i\mathbf{k}_{2\perp} \cdot \mathbf{y}_{\perp}}$$

Dijet cross-section in the CGC will contain dipoles and quadrupole:

$$\frac{1}{N_c} \langle \text{Tr} [V(\mathbf{x}_{\perp})V^{\dagger}(\mathbf{y}_{\perp})] \rangle_Y$$

$$\frac{1}{N_c} \langle \text{Tr} [V(\mathbf{x}_{\perp})V^{\dagger}(\mathbf{y}_{\perp})V(\mathbf{y}'_{\perp})V^{\dagger}(\mathbf{x}'_{\perp})] \rangle_Y$$

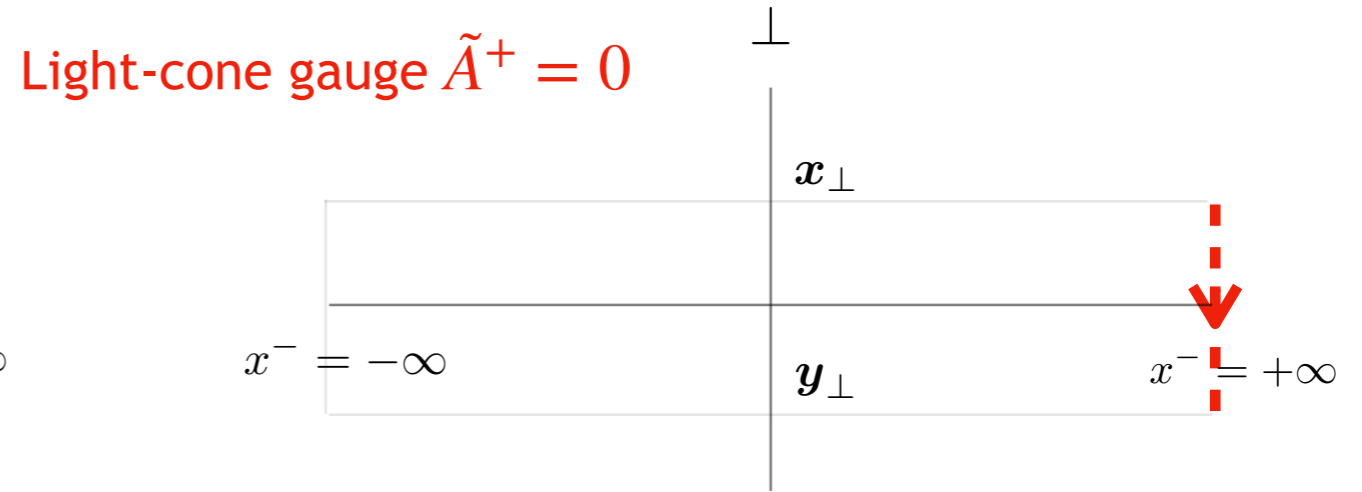
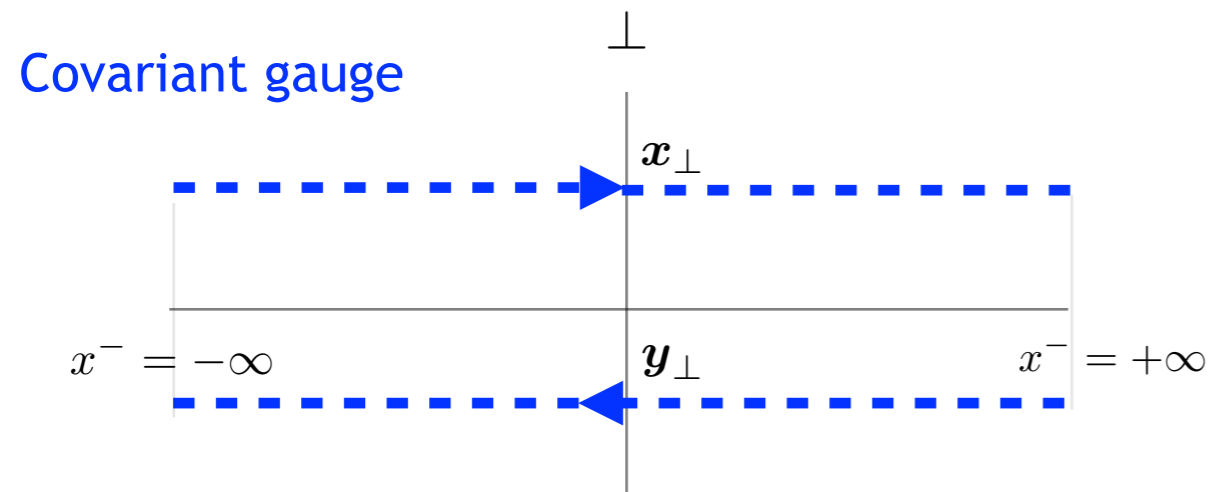
Building blocks of CGC observables!

Dijet production beyond TMDs

Choosing the gauge: light-like Wilson lines vs transverse gauge link

Boussarie, Mehtar-Tani (2020)

Pair of Wilson lines as transverse gauge link



$$V(\mathbf{x}_\perp)V^\dagger(\mathbf{y}_\perp) = \mathcal{P} \exp \left[-ig \int_{\mathbf{y}_\perp}^{\mathbf{x}_\perp} d\mathbf{z}_\perp \cdot \tilde{\mathbf{A}}_\perp(\mathbf{z}_\perp) \right]$$

gA expansion:

$$= 1 - ig \int_{\mathbf{y}_\perp}^{\mathbf{x}_\perp} d\mathbf{z}_\perp \cdot \tilde{\mathbf{A}}_\perp(\mathbf{z}_\perp) + \dots$$

Small dipole expansion:

$$= 1 + ig \mathbf{r}_\perp \cdot \tilde{\mathbf{A}}_\perp(\mathbf{z}_\perp) + \dots$$

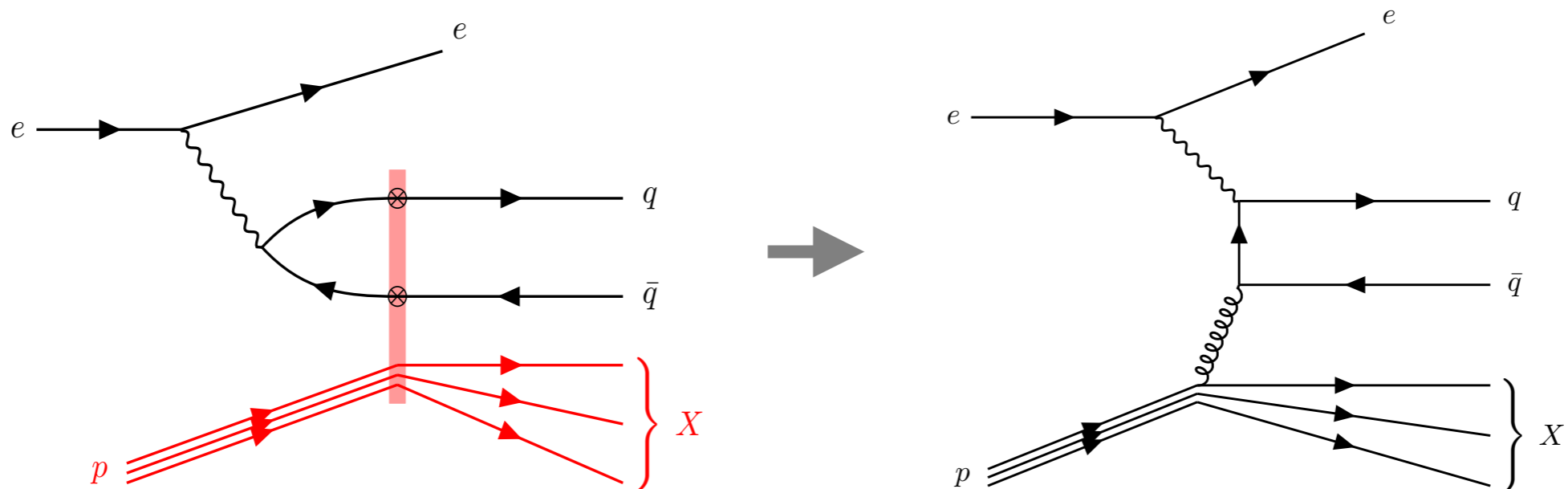
Altinoluk, Boussarie, Kotko (2019)

$$\mathbf{r}_\perp = \mathbf{x}_\perp - \mathbf{y}_\perp$$

Dominguez, Marquet, Xiao, Yuan (2011)

Dijet production beyond TMDs

From CGC to Improved TMD



CGC

$$V(\mathbf{x}_\perp)V^\dagger(\mathbf{y}_\perp) = \mathcal{P} \exp \left[-ig \int_{\mathbf{y}_\perp}^{\mathbf{x}_\perp} d\mathbf{z}_\perp \cdot \tilde{\mathbf{A}}_\perp(\mathbf{z}_\perp) \right]$$

Boussarie, Mehtar-Tani (2020)

Improved TMD

$$= 1 - ig \int_{\mathbf{y}_\perp}^{\mathbf{x}_\perp} d\mathbf{z}_\perp \cdot \tilde{\mathbf{A}}_\perp(\mathbf{z}_\perp) + \dots$$

TMD

Altinoluk, Boussarie, Kotko (2019)

$$= 1 + ig \mathbf{r}_\perp \cdot \tilde{\mathbf{A}}_\perp(\mathbf{z}_\perp) + \dots$$

$$\mathbf{r}_\perp = \mathbf{x}_\perp - \mathbf{y}_\perp$$

Dominguez, Marquet, Xiao, Yuan (2011)

Dijet production beyond TMDs

Resummation of power corrections and genuine saturation corrections

$$d\sigma_{\text{CGC}} = \underbrace{d\sigma_{\text{TMD}}}_{\text{d}\sigma_{\text{ITMD}}} + \overbrace{\mathcal{O}\left(\frac{k_{\perp}}{Q_{\perp}}\right)}^{\text{kinematic}} + \overbrace{\mathcal{O}\left(\frac{Q_s}{Q_{\perp}}\right)}^{\text{genuine}}$$

Dominguez, Marquet, Xiao, Yuan (2011)

TMD valid $k_{\perp}, Q_s \ll Q_{\perp}$

back-to-back hadrons/jets
and transverse momenta larger
than sat scale

Hard factor Weizsäcker-Williams gluon TMD

$$d\sigma^{\gamma^* A \rightarrow q\bar{q}X} \sim \mathcal{H}_{\text{TMD}}^{ij}(\mathbf{P}_{\perp}) \alpha_s x G_{\text{WW}}^{ij}(x, \mathbf{k}_{\perp}) + \mathcal{O}(k_{\perp}/P_{\perp}) + \mathcal{O}(Q_s/P_{\perp})$$

Altinoluk, Boussarie, Kotko (2019)

For massive quarks see Altinoluk, Marquet, Taelis. (2021)

Improved TMD valid $Q_s \ll Q_{\perp}$

transverse momenta larger
than sat scale

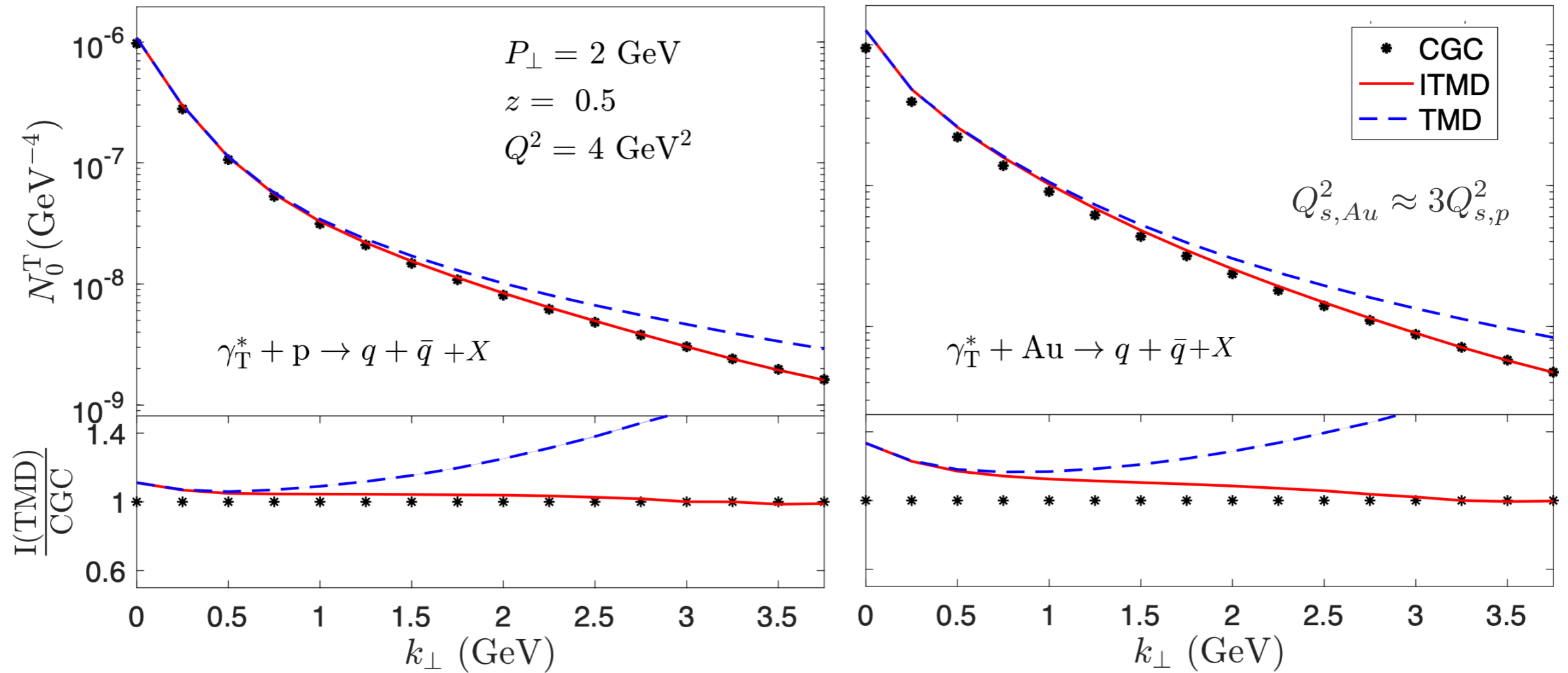
Hard factor resums
kinematic powers k_{\perp}/P_{\perp}

$$d\sigma^{\gamma_{\lambda}^* A \rightarrow q\bar{q}X} \sim \mathcal{H}_{\text{ITMD}}^{\lambda, ij}(\mathbf{P}_{\perp}, \mathbf{k}_{\perp}) \alpha_s x G_{\text{WW}}^{ij}(x, \mathbf{k}_{\perp}) + \mathcal{O}(Q_s/P_{\perp})$$

See Krzysztof's talk for more
on ITMD at the EIC!

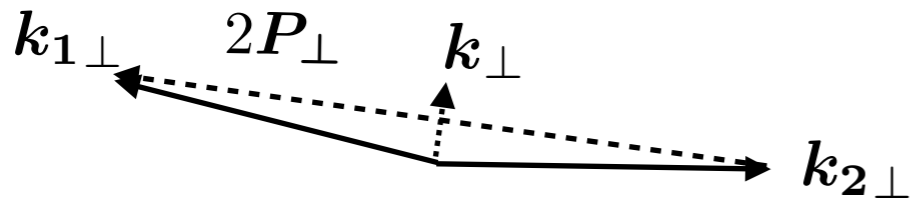
Dijet production beyond TMDs

Differential yield: TMD, ITMD and CGC



proton ~ smaller Q_s^2

Gold nucleus ~ larger Q_s^2



$$\frac{dN_{\gamma_\lambda^* + A \rightarrow q\bar{q} + X}}{d^2\mathbf{P}_\perp d^2\mathbf{k}_\perp d\eta_1 d\eta_2} = N_0^\lambda(P_\perp, k_\perp) \left[1 + 2 \sum_{k=1}^{\infty} v_{k,\lambda}(P_\perp, k_\perp) \cos(k\phi) \right]$$

$$\phi \equiv \phi_{\mathbf{k}_\perp} - \phi_{\mathbf{P}_\perp}$$

R. Boussarie, H. Mäntysaari, FS, B. Schenke (2021)

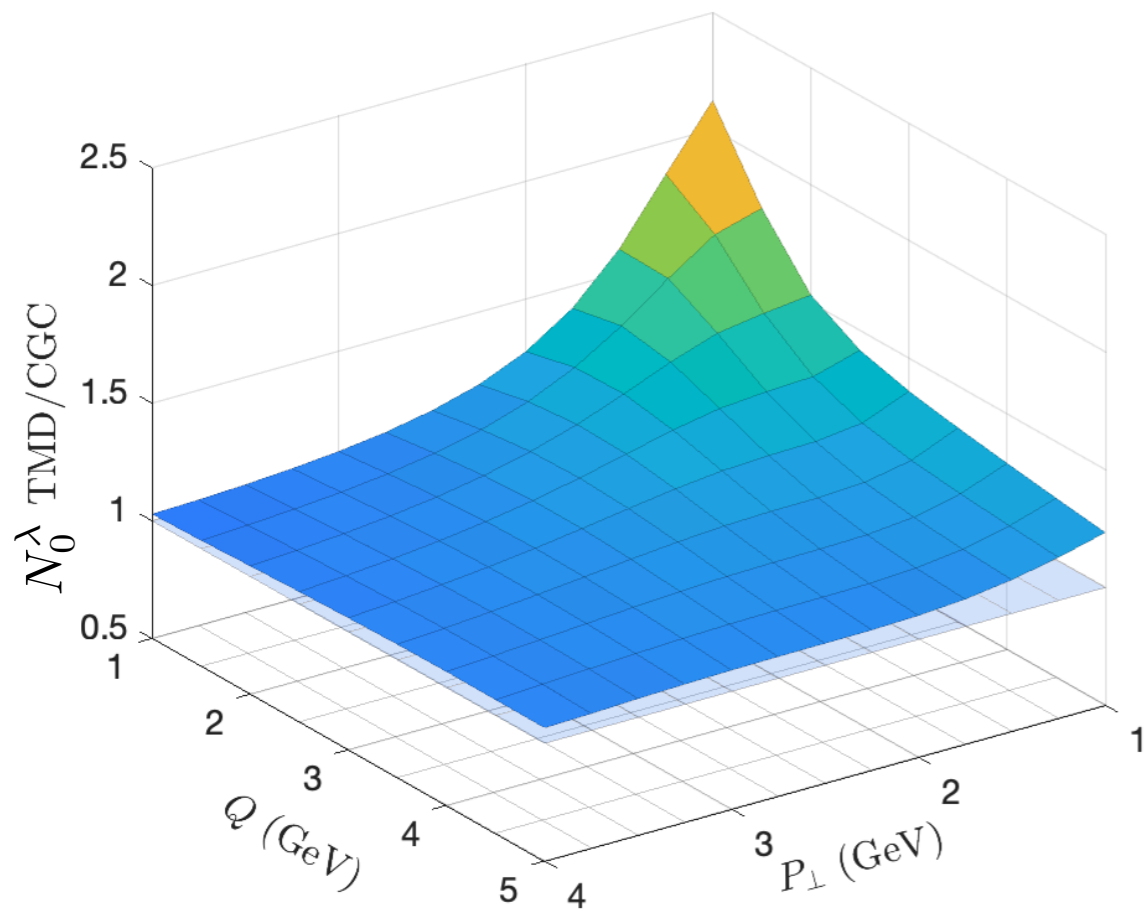
For a comparison of TMD, ITMD and CGC in pA see Fuji, Watanabe, Marquet (2020)

Dijet production beyond TMDs

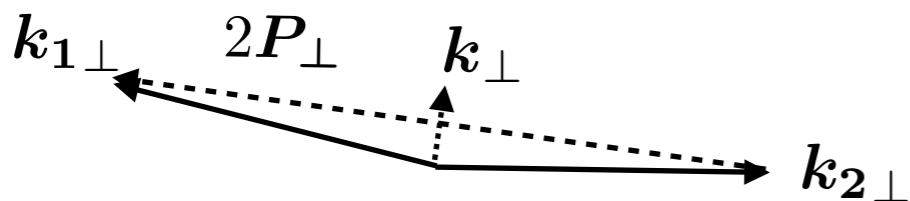
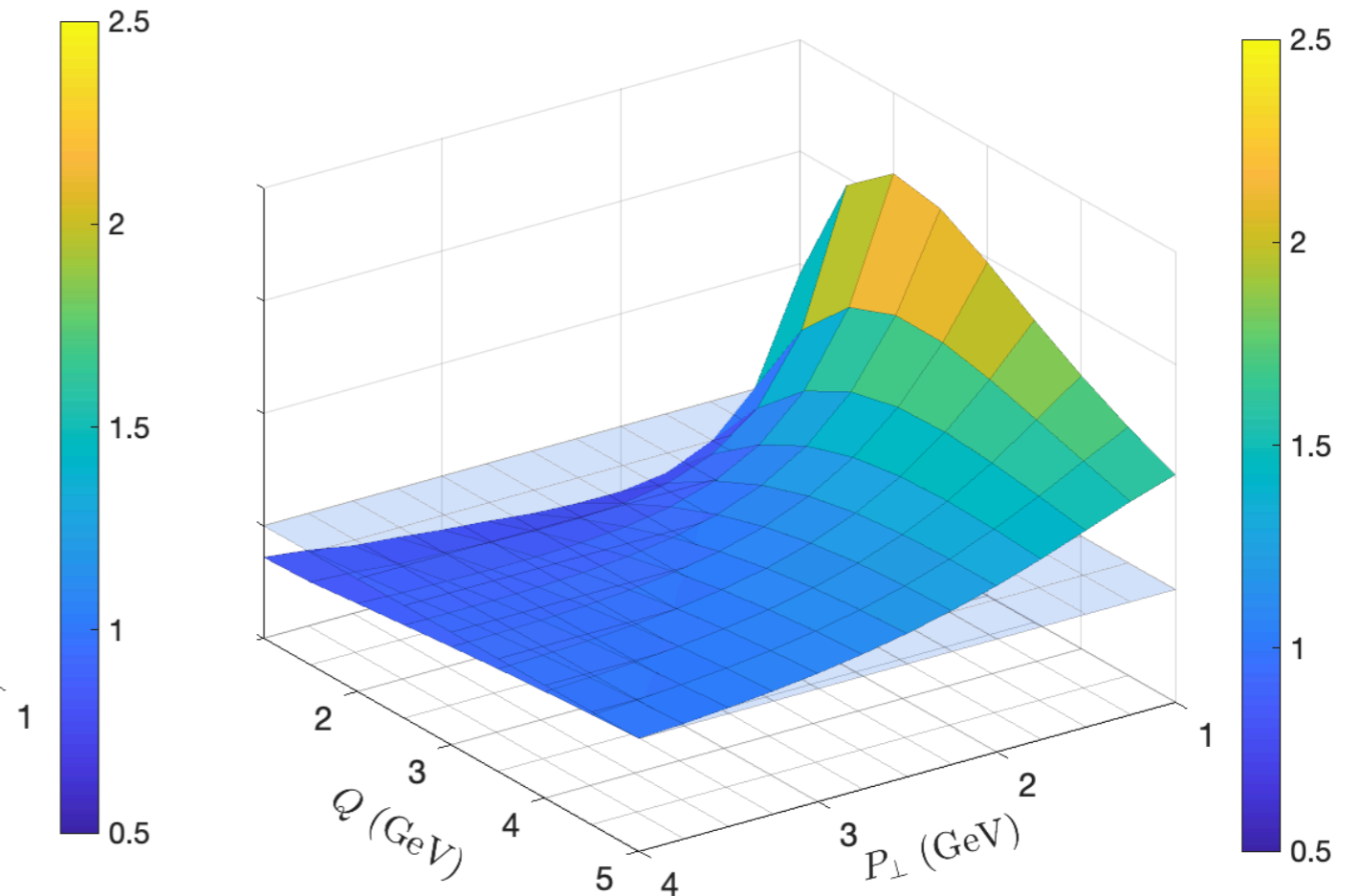
Q^2 and P_\perp dependence of genuine saturation

At exactly back-to-back $k_\perp \approx 0$ the ratio of CGC/TMD is sensitive to genuine twists

$$\gamma_T^* + \text{Au} \rightarrow q + \bar{q} + X$$



$$\gamma_L^* + \text{Au} \rightarrow q + \bar{q} + X$$

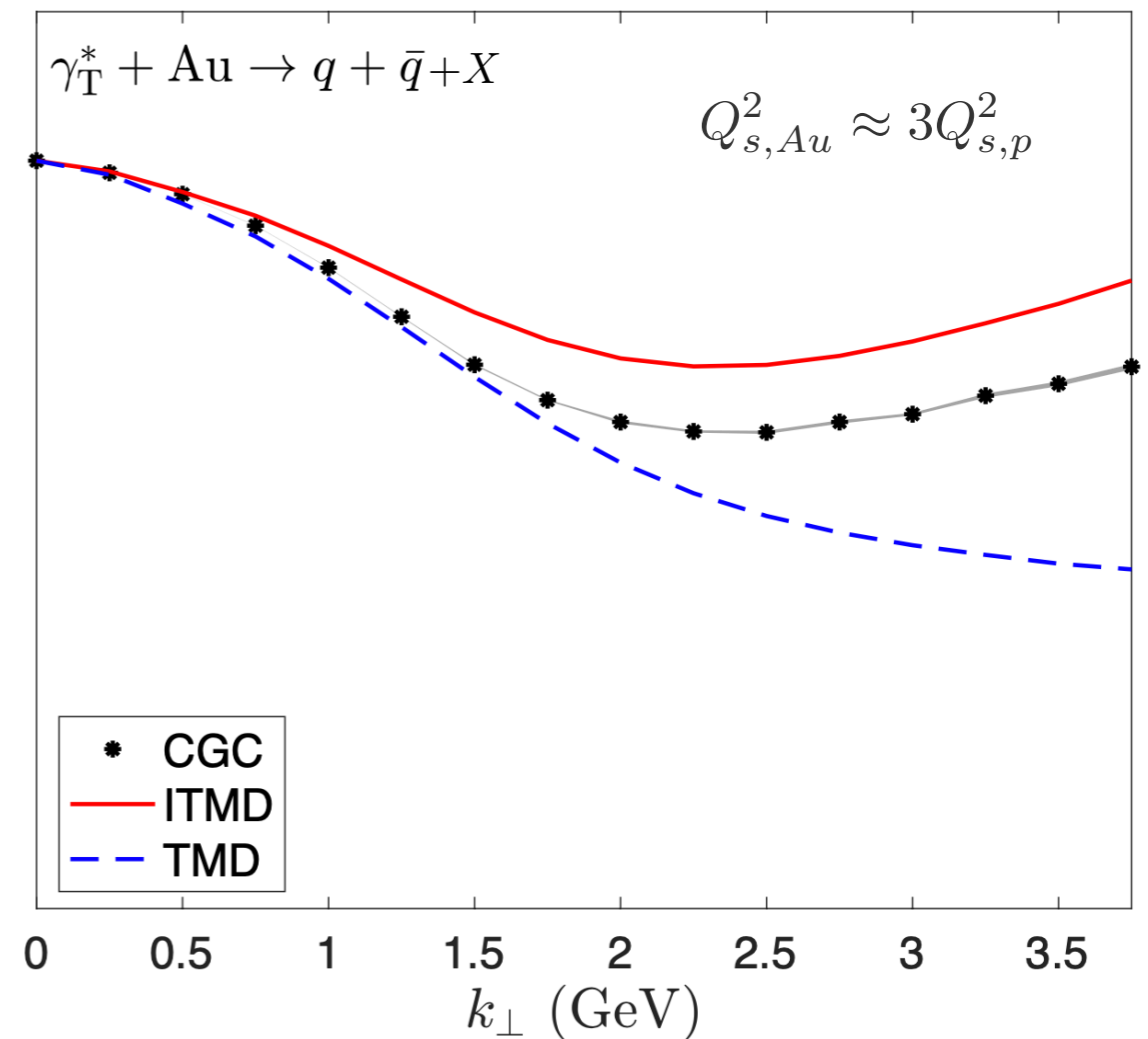
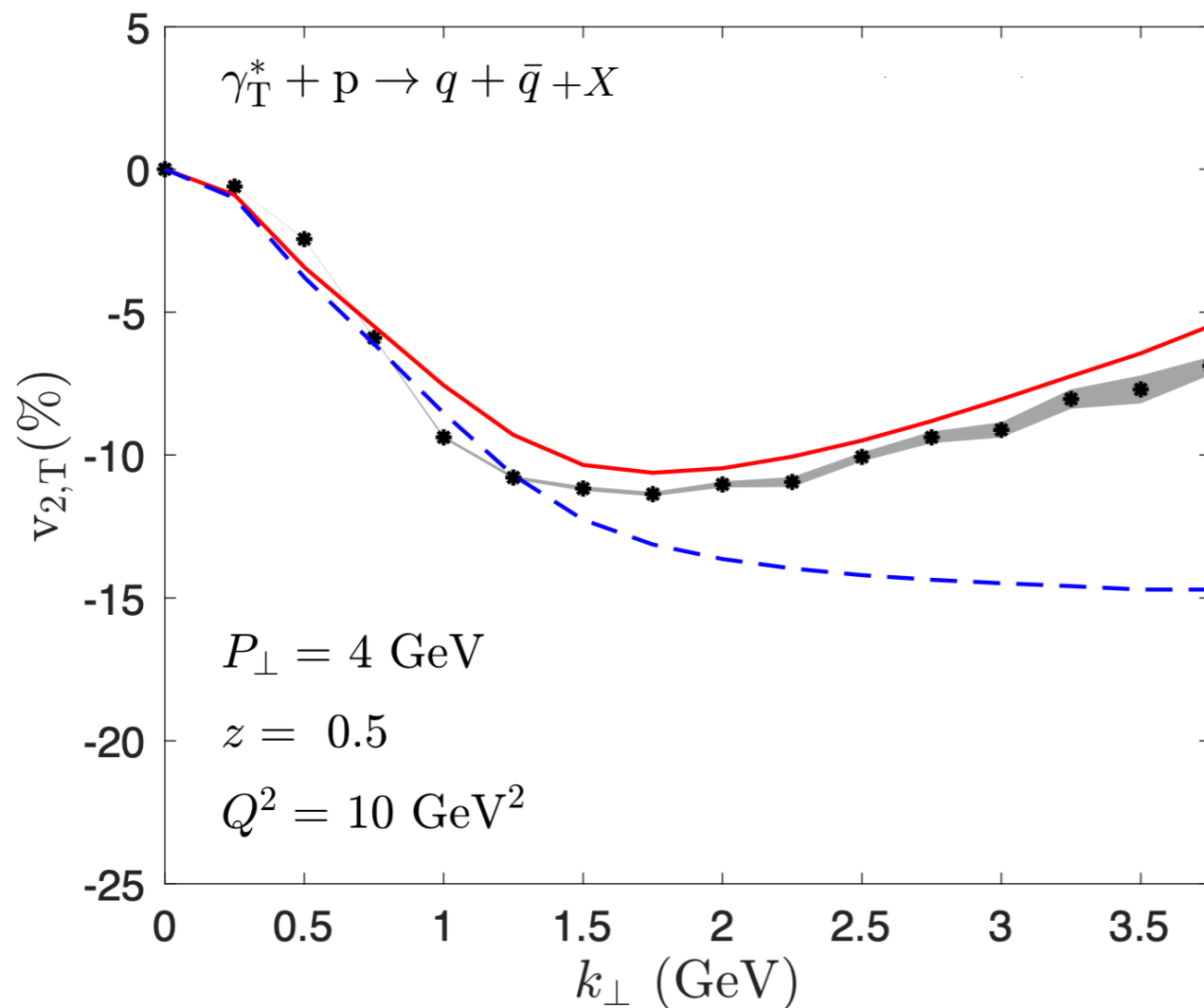


$$\frac{dN_{\gamma_\lambda^* + A \rightarrow q\bar{q} + X}}{d^2\mathbf{P}_\perp d^2\mathbf{k}_\perp d\eta_1 d\eta_2} = N_0^\lambda(P_\perp, k_\perp) \left[1 + 2 \sum_{k=1}^{\infty} v_{k,\lambda}(P_\perp, k_\perp) \cos(k\phi) \right]$$

$$\phi \equiv \phi_{\mathbf{k}_\perp} - \phi_{\mathbf{P}_\perp}$$

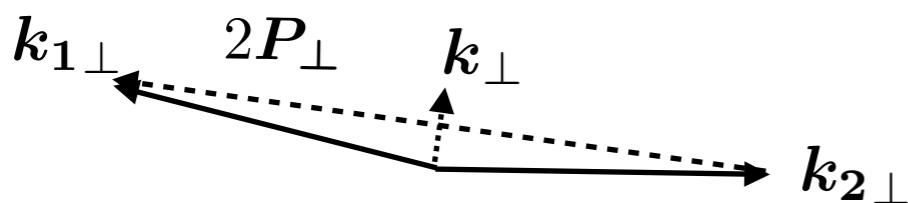
Dijet production beyond TMDs

Momentum imbalance elliptic anisotropies:
TMD vs ITMD vs CGC



proton ~ smaller Q_s^2

Gold nucleus ~ larger Q_s^2

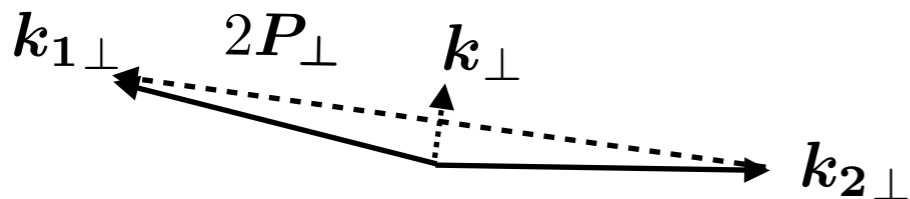
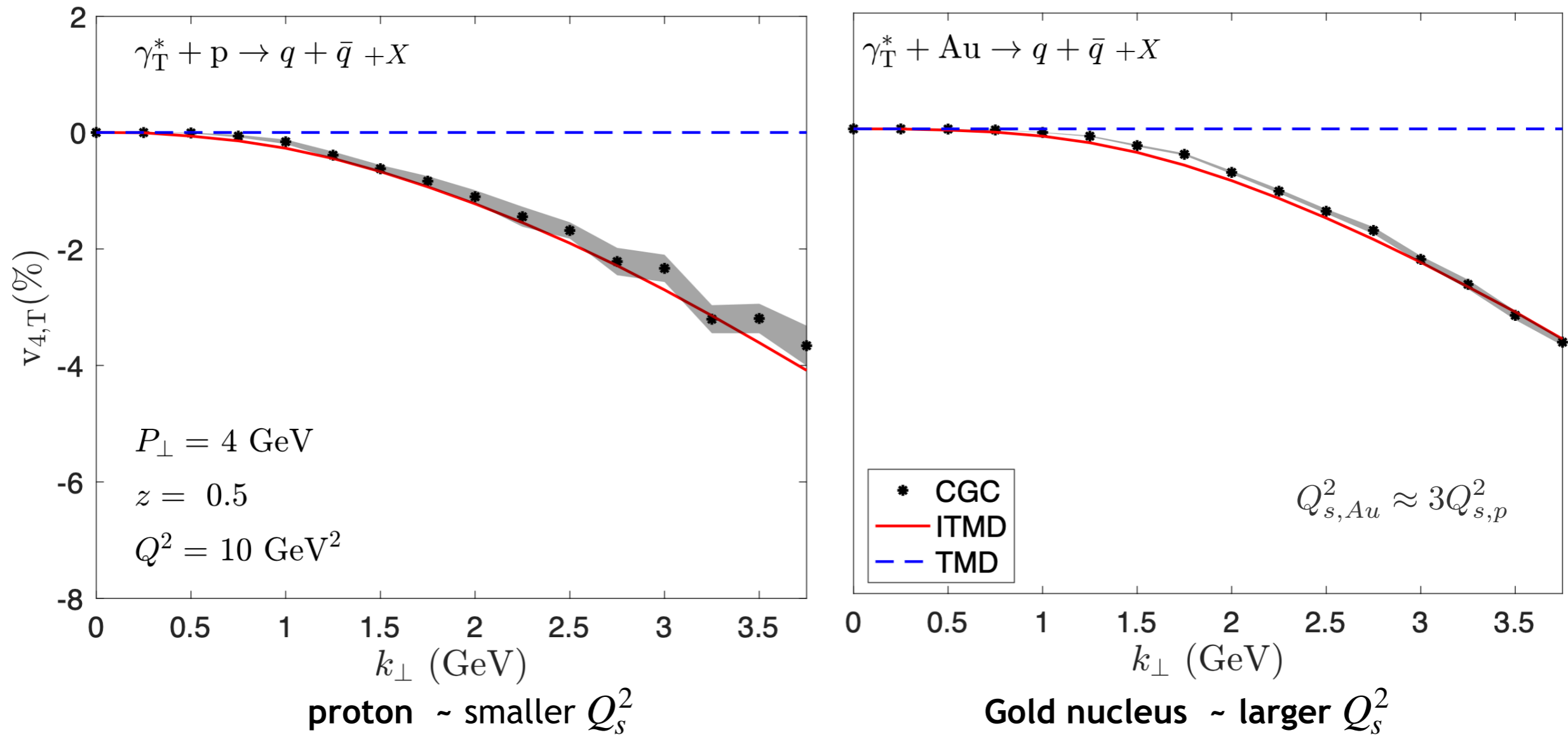


$$\frac{dN^{\gamma^*+A \rightarrow q\bar{q}+X}}{d^2\mathbf{P}_\perp d^2\mathbf{k}_\perp d\eta_1 d\eta_2} = N_0^\lambda(P_\perp, k_\perp) \left[1 + 2 \sum_{k=1}^{\infty} v_{k,\lambda}(P_\perp, k_\perp) \cos(k\phi) \right]$$

$$\phi \equiv \phi_{\mathbf{k}_\perp} - \phi_{\mathbf{P}_\perp}$$

Dijet production beyond TMDs

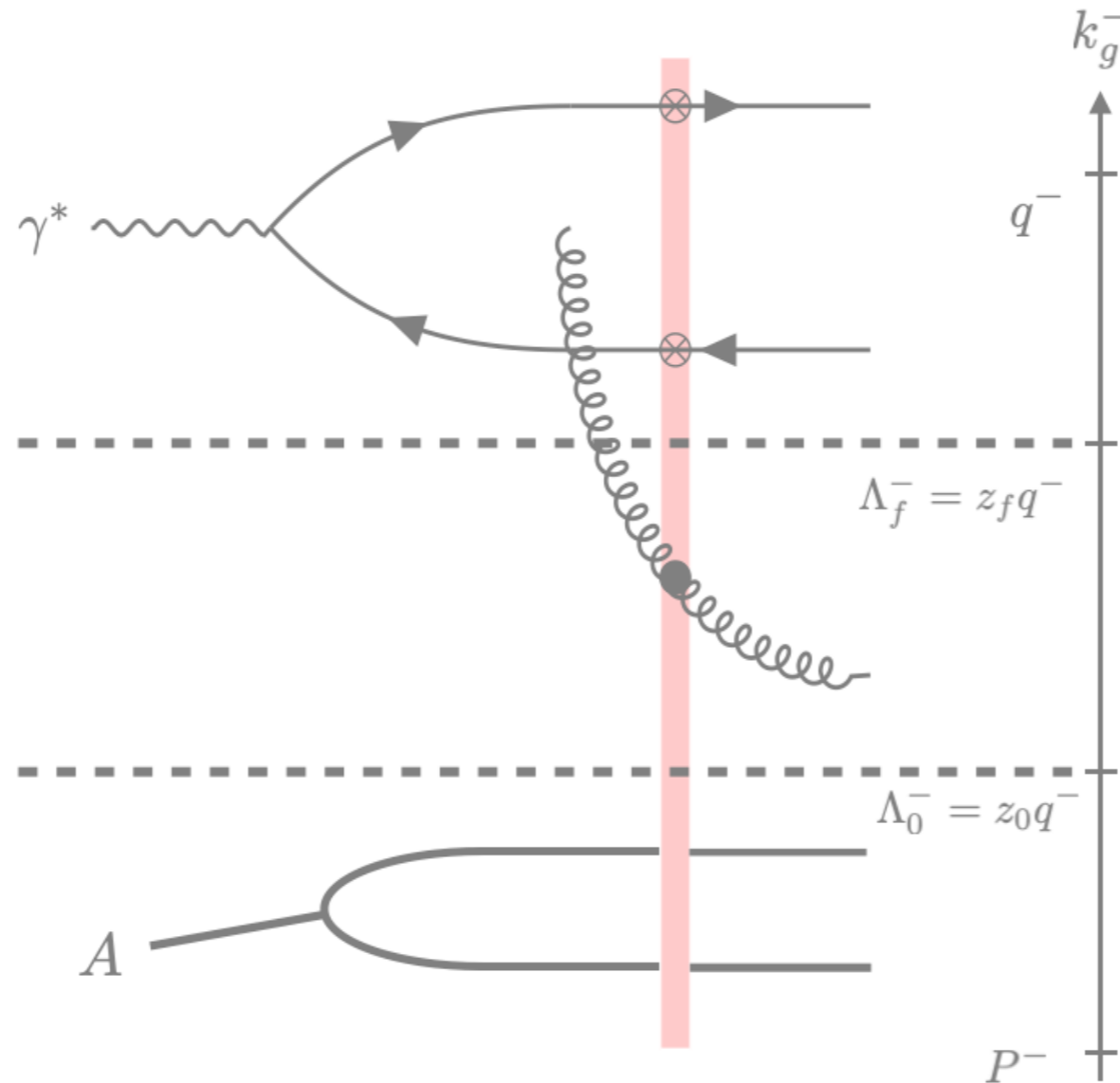
Momentum imbalance quadrangular anisotropies:
TMD vs ITMD vs CGC



$$\frac{dN^{\gamma_\lambda^* + A \rightarrow q\bar{q} + X}}{d^2\mathbf{P}_\perp d^2\mathbf{k}_\perp d\eta_1 d\eta_2} = N_0^\lambda(P_\perp, k_\perp) \left[1 + 2 \sum_{k=1}^{\infty} v_{k,\lambda}(P_\perp, k_\perp) \cos(k\phi) \right]$$

$$\phi \equiv \phi_{\mathbf{k}_\perp} - \phi_{\mathbf{P}_\perp}$$

Dijet production in the CGC at NLO



Rapidity factorization and NLO impact factor

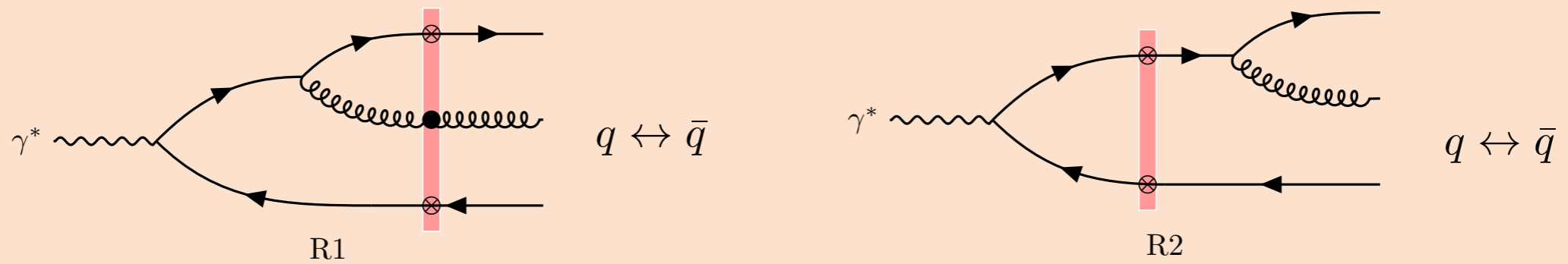
P. Caucal, FS, and R. Venugopalan. [2108.06347](#)
(To appear on JHEP)



Dijet production in the CGC at NLO

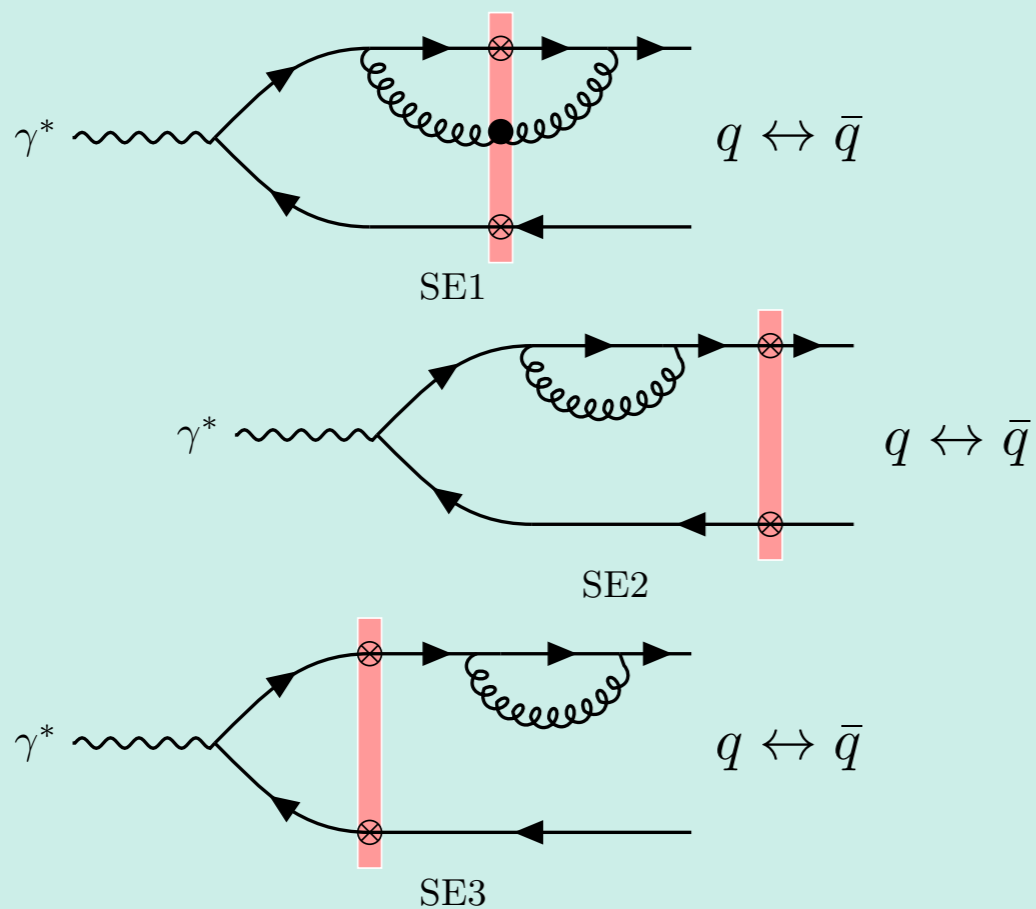
Real and virtual emissions

Real emission diagrams (loop opens in DA and closes in the CCA)

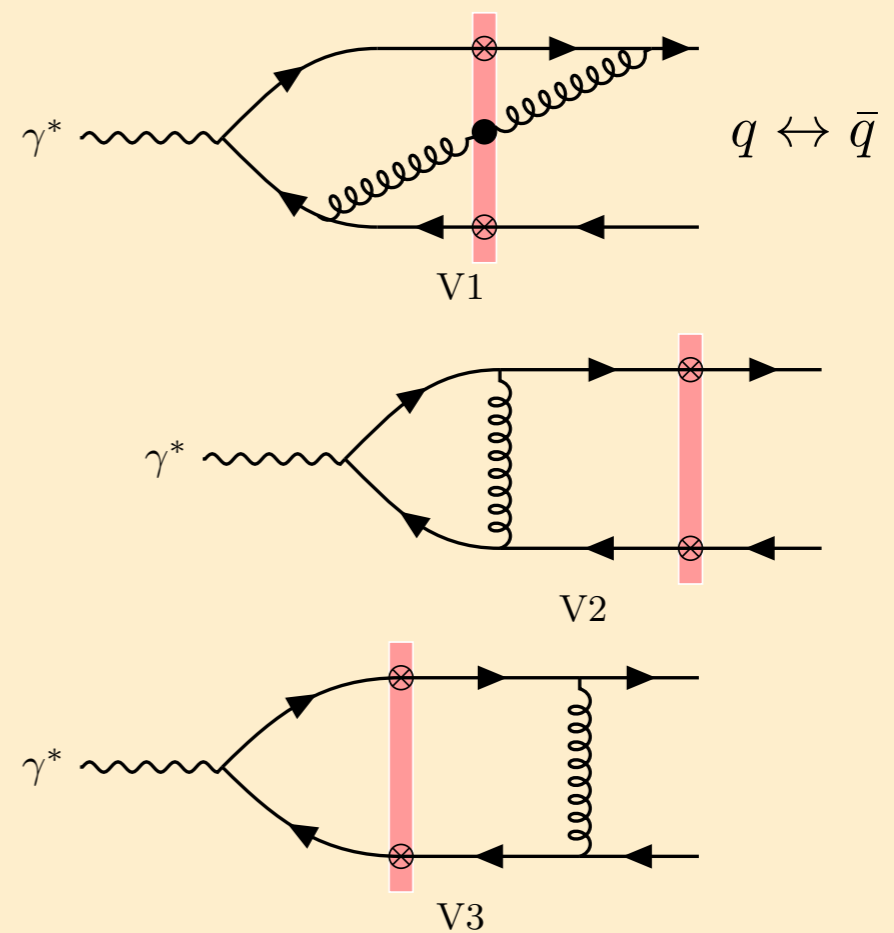


Virtual emission (loop open and closes in DA or CCA)

Self-energy contributions



Vertex contributions



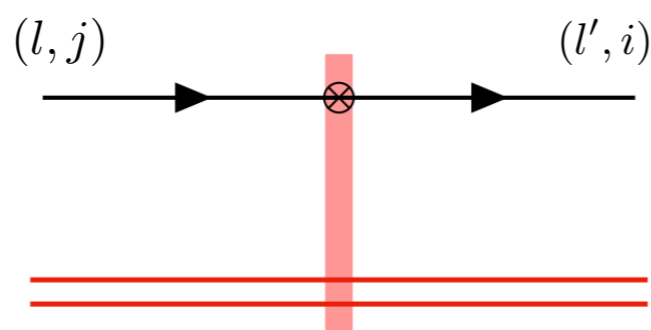
Dijet production in the CGC at NLO

Setup for the calculation

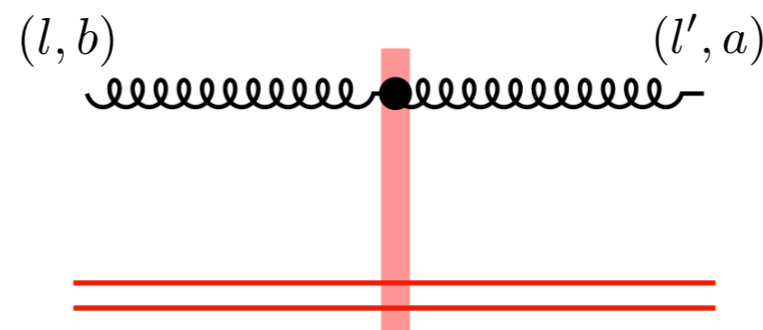
- Covariant perturbation theory in momentum space (another popular approach is LCPT)

Standard QED, QCD rules: propagators, vertices, polarization vectors, etc

- Vertices for (eikinally) coupling to the CGC background field (in $A_{c1}^- = 0$ gauge)



$$\mathcal{T}_{ij}^q(l, l') = (2\pi)\delta(l^- - l'^-)\gamma^- \text{sgn}(l^-) \times \int d^2z_\perp e^{-i(l'_\perp - l_\perp) \cdot z_\perp} V_{ij}^{\text{sgn}(l^-)}(z_\perp)$$



$$\mathcal{T}_{ab}^g(l, l') = -(2\pi)\delta(l^- - l'^-)(2l^-)g_{\mu\nu} \text{sgn}(l^-) \times \int d^2z_\perp e^{-i(l'_\perp - l_\perp) \cdot z_\perp} U_{ab}^{\text{sgn}(l^-)}(z_\perp)$$

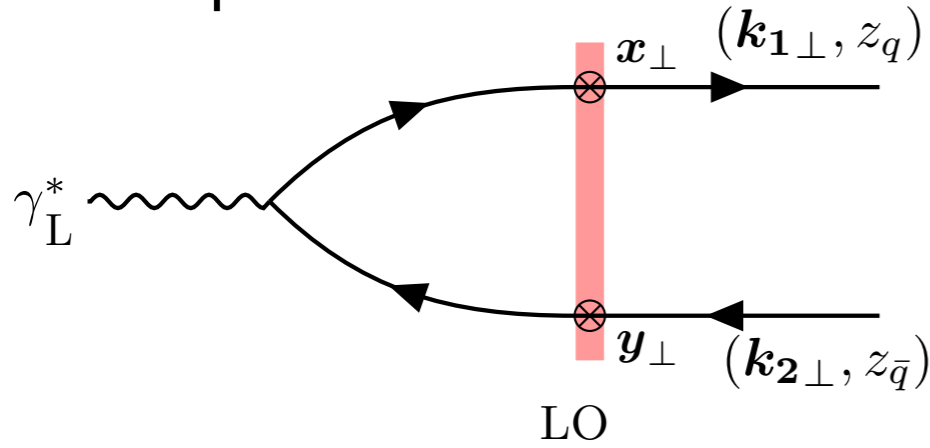
- Regularization schemes

dimensional regularization + rapidity cut-off

Dijet production in the CGC at NLO

An example of structure of LO vs NLO amplitudes

LO amplitude



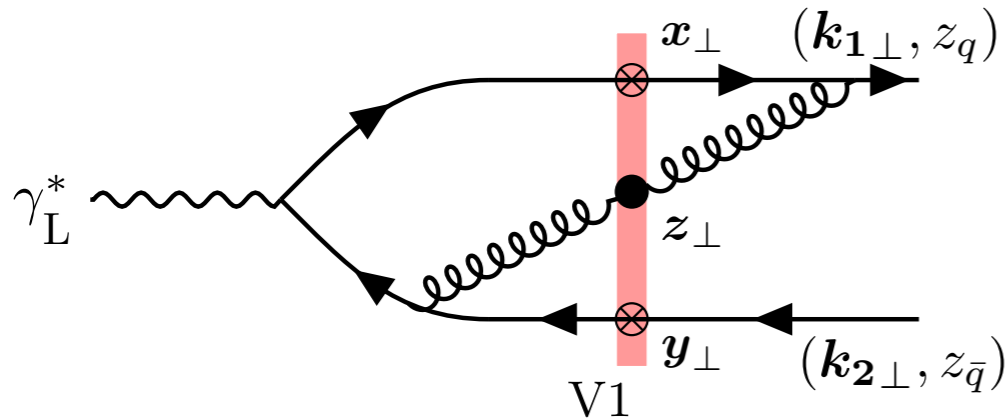
$$\otimes_{\text{LO}} \equiv \frac{eefq^-}{\pi} \int d^2\mathbf{x}_\perp d^2\mathbf{y}_\perp e^{-i\mathbf{k}_{1\perp} \cdot \mathbf{x}_\perp} e^{-i\mathbf{k}_{2\perp} \cdot \mathbf{y}_\perp}$$

$$X_{q\bar{q}}^2 = z_q z_{\bar{q}} r_{xy}^2 \quad \text{effective dipole size}$$

$$\mathcal{M}_{\text{LO}}^{L,\sigma\sigma'} = \left[1 - V(\mathbf{x}_\perp) V^\dagger(\mathbf{y}_\perp) \right] \otimes_{\text{LO}} 2(z_q z_{\bar{q}})^{3/2} Q K_0(Q X_{q\bar{q}}) \delta^{\sigma, -\sigma'}$$

non-perturbative perturbatively computable

Dressed vertex amplitude



$$\otimes_{\text{V}} \equiv \frac{eefq^-}{\pi} \int d^2\mathbf{x}_\perp d^2\mathbf{y}_\perp d^2\mathbf{z}_\perp e^{-i\mathbf{k}_{1\perp} \cdot \mathbf{x}_\perp} e^{-i\mathbf{k}_{2\perp} \cdot \mathbf{y}_\perp}$$

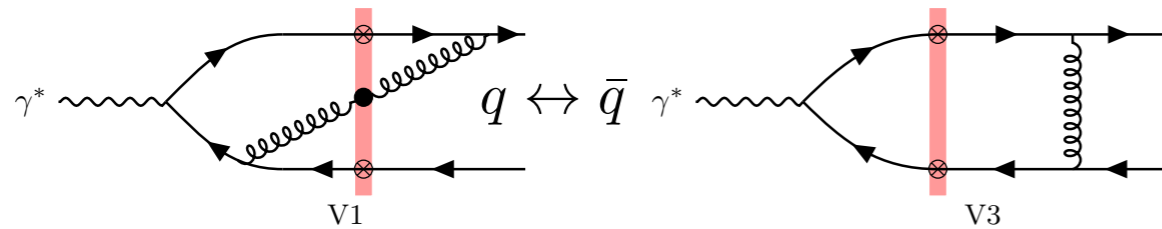
$$X_{q\bar{q}g}^2 = (z_q - z_g) z_{\bar{q}} r_{xy}^2 + (z_q - z_g) z_g r_{xz}^2 + z_g z_{\bar{q}} r_{zy}^2 \quad \text{effective dipole size}$$

$$\mathcal{M}_{\text{V1}}^{L,\sigma\sigma'} = \left[C_F \mathbb{1} - t^a V(\mathbf{x}_\perp) t^b V^\dagger(\mathbf{y}_\perp) U_{ab}(z_\perp) \right] \otimes_{\text{V}} \frac{\alpha_s}{\pi^2} \int_{z_0}^{z_q} \frac{dz_g}{z_g} \frac{\mathbf{r}_{zx} \cdot \mathbf{r}_{zy}}{\mathbf{r}_{zx}^2 \mathbf{r}_{zy}^2} \left[\left(1 - \frac{z_g}{z_q}\right) \left(1 + \frac{z_g}{z_{\bar{q}}}\right) \left(1 - \frac{z_g}{2z_q} - \frac{z_g}{2(z_{\bar{q}} + z_g)}\right) + \dots \right] e^{-i\frac{z_g}{z_q} \mathbf{k}_\perp \cdot \mathbf{r}_{zx}}$$

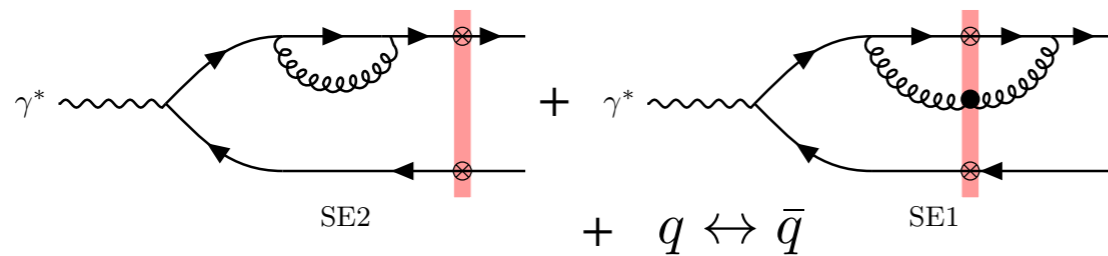
non-perturbative perturbatively computable

Dijet production in the CGC at NLO

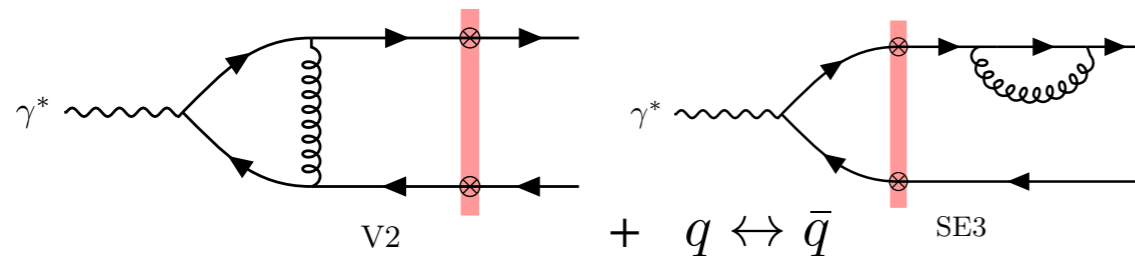
Cancellation of divergences of UV divergences



- UV finite diagrams



- UV divergences cancel among self energies contributions (before SW and crossing SW)

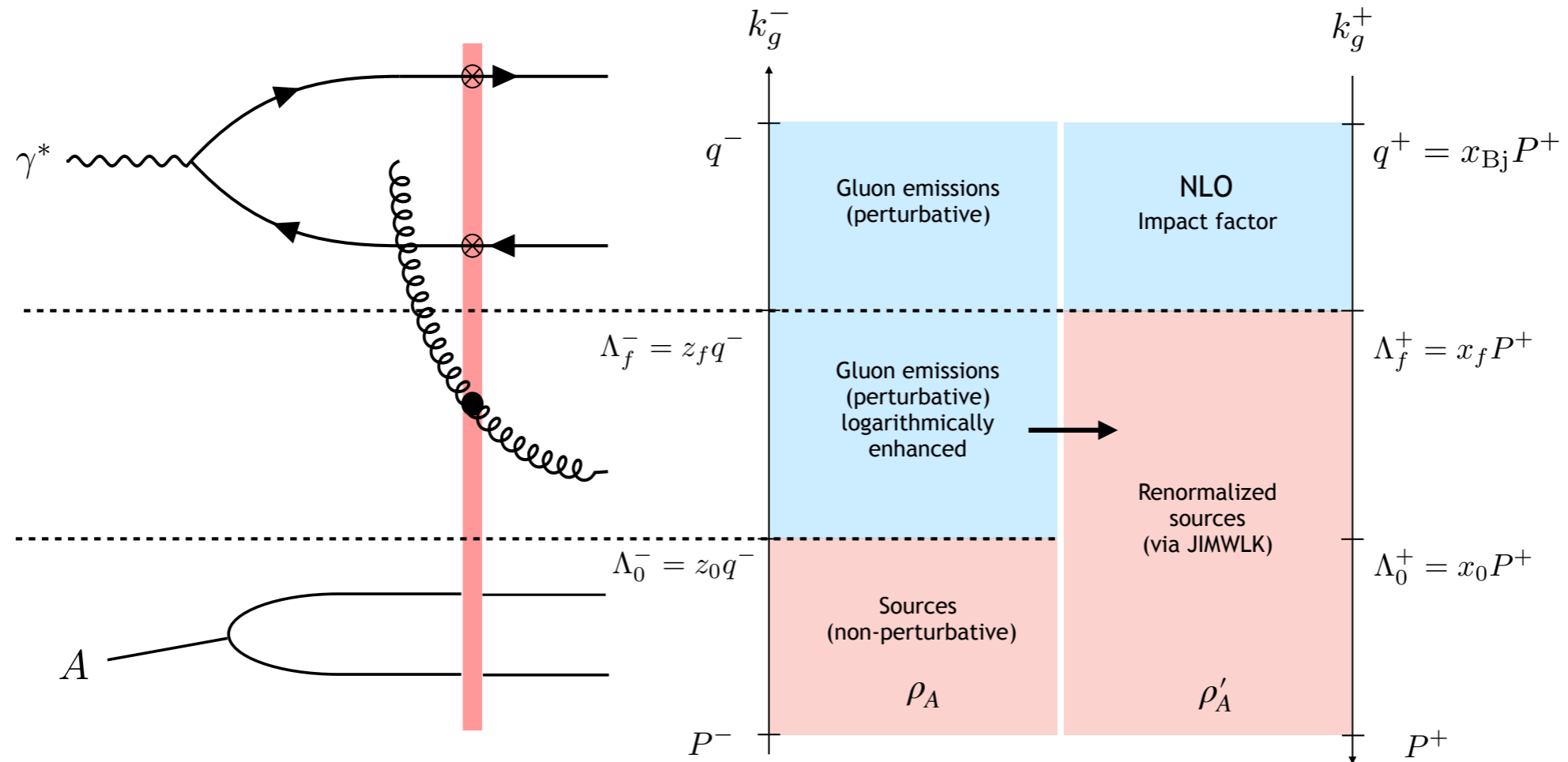


- UV divergence cancel in vertex contribution before SW and self energy contribution after SW

- UV finite, no need for counter-terms at this order in PT.
- Overall IR divergence is left in sum of virtual diagrams, and soft divergence left in V3. Both cancel with real emissions.

Inclusive dijet production at NLO

Rapidity (slow gluon) divergences and JIMWLK factorization



**JIMWLK LL
Hamiltonian**

$$d\sigma_{\text{NLO}} = \alpha_s \ln \left(\frac{z_f}{z_0} \right) \mathcal{H}_{\text{LL}} d\sigma_{\text{LO}} + \alpha_s d\sigma_{\text{NLO}, \text{i.f.}}$$

Large logs need to be resummed!

Evolution of sources (weight functional)

$$\alpha_s \ln \left(\frac{z_f}{z_0} \right) \sim \alpha_s \ln (s)$$

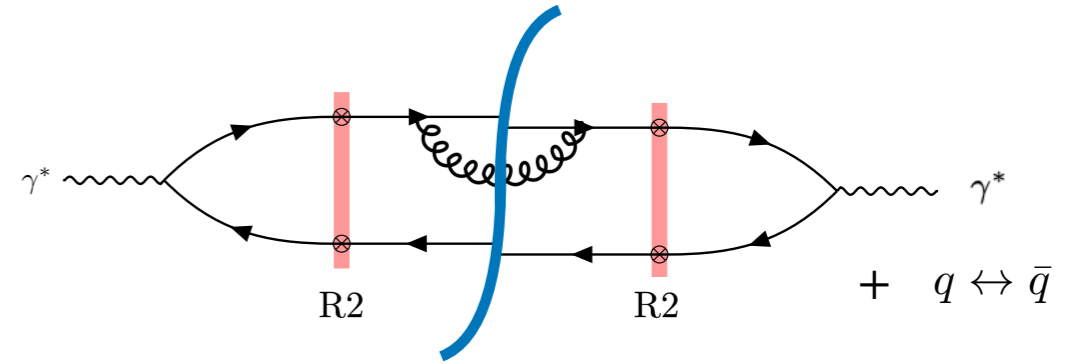
$$W_{\Lambda_0^-} [\rho_A] \rightarrow W_{\Lambda_f^-} [\rho'_A]$$

Dijet production in the CGC at NLO

Infrared and collinear safety

Collinear non-slow divergences

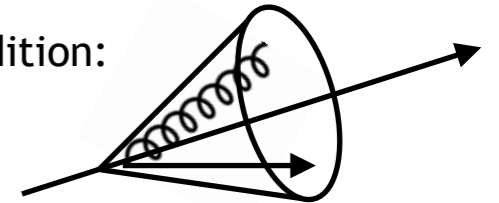
- Implement a jet algorithm* (small cone) excluding slow gluon divergence



Phase space for collinear non-slow gluon

$$\int_{z_f}^{z_j} \frac{dz_g}{z_g} \mu^\epsilon \int \frac{d^{2-\epsilon} \mathcal{C}_{qg,\perp}}{(2\pi)^{2-\epsilon}} \frac{1}{\mathcal{C}_{qg,\perp}^2}$$

Small-cone condition:

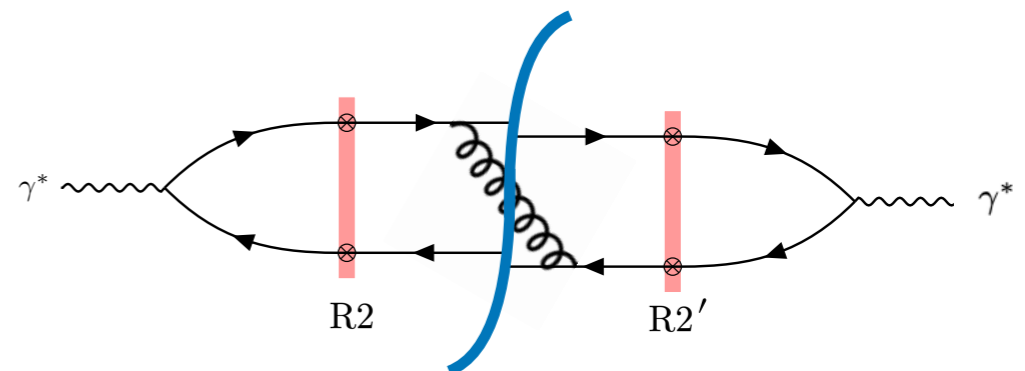
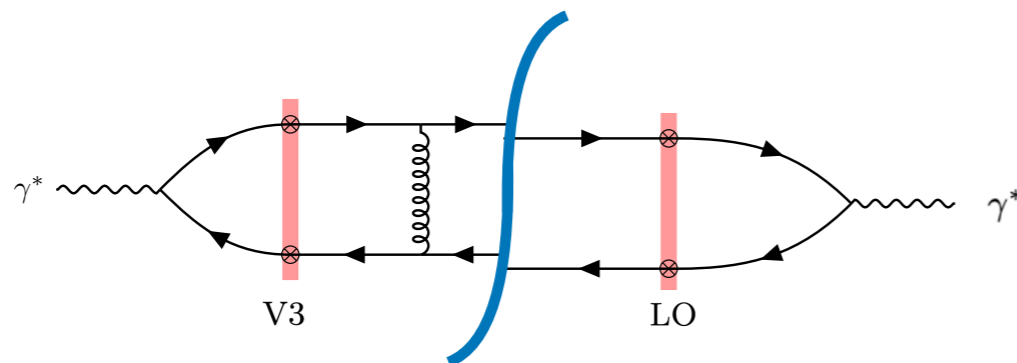


- Collinear divergence cancels against IR divergence left in virtual contributions

$$\mathcal{C}_{qg,\perp}^2 \leq \mathcal{C}_{qg,\perp}^2|_{\max} = R^2 p_j^2 \min \left(\frac{z_g^2}{z_j^2}, \frac{(z_j - z_g)^2}{z_j^2} \right)$$

Soft divergence

- Remaining soft divergence cancel between vertex correction after SW, and cross term real gluon emission after SW



Summary

- Dijet production in the TMD formalism
Observables at the EIC
- Dijet production at EIC beyond TMDs
Resummation of kinematic and genuine saturation corrections
- Dijet production at EIC in the CGC at NLO
JIMWLK rapidity factorization, and finite impact factor

Outlook

- Couple our partonic cross-sections to event generators

How much of the kinematic power and genuine saturation corrections survives in the actual observable?

- Investigate dijet production at NLO in the back-to-back limit

Match to TMD factorization at NLO

Xiao, Yuan, Zhou (2017)
Hentschinski (2021)

See Martin's talk for
high energy
factorization at NLO!

Is the Improved TMD framework valid at NLO?

- Numerical implementation of dijet production at NLO

Promoting saturation physics to a precision science

- Employ modern techniques such SCET to the CGC at NLO

Extend existing SCET studies for dijet TMD factorization to the small- x regime

del Castillo, Echevarria, Makris, Scimemi (2020)
Kang, Reiten, Shao, Terry (2020)